Solid-State ^{51}V NMR and Infrared Spectroscopic Study of Vanadium Oxide Supported on TiO_2-ZrO_2

Eun Hee Park, Man Ho Lee, and Jong Rack Sohn[*]

Dept. of Industrial Chemistry, Engineering College, Kyungpook National University, Taegu 702-701, Korea
Received May 15, 2000

Vanadium oxide catalyst supported on TiO_2-ZrO_2 has been prepared by adding $Ti(OH)_4$-$Zr(OH)_4$ powder to an aqueous solution of ammonium metavanadate followed by drying and calcining at high temperatures. The characterization of the prepared catalysts was performed using solid-state ^{51}V NMR and FTIR. In the case of calcination temperature at 773 K, vanadium oxide was in a highly dispersed state for the samples containing low loading V_2O_5 below 25 wt %, but for samples containing high loading V_2O_5 equal to or above 25 wt %, vanadium oxide was well crystallized due to the V_2O_5 loading exceeding the formation of monolayer on the surface of TiO_2-ZrO_2. The ZrV_2O_7 compound was formed through the reaction of V_2O_5 and ZrO_2 at 773-973 K, whereas the $V_3Ti_6O_{17}$ compound was formed through the reaction of V_2O_5 and TiO_2 at 973-1073 K. The $V_3Ti_6O_{17}$ compound decomposed to V_2O_5 and TiO_2 at 1173 K, which were confirmed by FTIR and ^{51}V NMR.

Introduction

Vanadium oxides are widely used as catalysts in oxidation reactions, *e.g.*, the oxidation of sulfur dioxide, carbon monoxide, and hydrocarbons.[1-5] These systems have also been found to be effective catalysts for the oxidation of methanol to methylformate.[6,7] Vanadia catalysts supported on titania-alumina mixed oxide and titania modified with alumina were found to exhibit superior activities in selective catalytic reduction of NOx.[8-11] Much research has been done to understand the nature of active sites, the surface structure of catalysts and the role played by the promoter of the supported catalysts, using infrared (IR), X-ray diffraction (XRD), electron spin resonance (E.S.R) and Raman spectroscopy.[7,12-14] Silica, titania, zirconia and alumina[15-22] have been commonly employed as vanadium oxide supports, and comparatively few studies have been reported on binary oxide TiO_2-ZrO_2 as a support for vanadium oxide.

It is well known that the dispersion and structural features of supported species can depend strongly on the support. The promoting effect of a TiO_2 support on the oxidation of o-xylene on V_2O_5 has been ascribed to an increase of the number of surface V=O bonds on the V_2O_5/TiO_2 catalysts and the weakening of these bonds.[23] In many studies concerning the mechanism involved in the catalytic reactions on vanadium oxide, the V=O species have been considered to play a significant role as active sites for the reactions.[24] Structure and other physicochemical properties of the supported metal oxides are considered to be in different states compared with bulk metal oxides because of their interaction with the supports. Solid-state nuclear magnetic resonance (NMR) methods represent a novel and promising approach to these systems. Since only the local environment of a nucleus under study is probed by NMR, this method is well suited for the structural analysis of disordered systems such as the two-dimensional surface vanadium oxide phases that is of particular interest in the present study. In addition

to the structural information provided by NMR methods, the direct proportionality of the signal intensity to the number of contributing nuclei makes NMR be useful for quantitative studies. In the present investigation, the techniques of solid-state ^{51}V NMR and Fourier transform infrared (FTIR) have been utilized to characterize a series of V_2O_5 samples supported on TiO_2-ZrO_2 with various vanadia loadings.

Experimental Section

Catalyst Preparation. The coprecipitate of $Ti(OH)_4$-$Zr(OH)_4$ was obtained by adding slowly aqueous ammonia into a mixed aqueous solution of titanium tetrachloride and zirconium oxychloride at room temperature with stirring until the pH of the mother liquor reached about 8. The ratio of titanium tetrachloride to zirconium oxychloride was 1 : 1. The coprecipitate thus obtained was washed thoroughly with distilled water until chloride ion was undetectable, and then dried at 383 K for 12 h. The dried coprecipitate was powdered below 100 mesh.

The catalysts containing various vanadium oxide content were prepared by adding the $Ti(OH)_4$-$Zr(OH)_4$ powder into an aqueous solution of ammonium metavanadate (NH_4VO_3) followed by drying and calcining at high temperatures for 3 h in air. This series of catalysts are denoted by their weight percentage of V_2O_5. For example, 10-V_2O_5/TiO_2-ZrO_2 indicates the catalyst containing 10 wt % V_2O_5.

Characterization. FTIR absorption spectra of V_2O_5/TiO_2-ZrO_2 powders were measured by the KBr disk method over the range 1200-400 cm^{-1}. The samples for the KBr disk method were prepared by grinding a mixture of the catalyst and KBr powders in an agate mortar and pressing them in the usual way. FTIR spectra of ammonia adsorbed on the catalyst were obtained in a heatable gas cell at room temperature using a Mattson Model GL 6030E spectrophotometer. The self-supporting catalyst wafers contained about 9 mg/cm^2. Before obtaining the spectra the samples were heated

under vacuum at 673-773 K for 2 h.

[51]V NMR spectra were measured by a Varian Unity Inova 300 spectrometer with a static magnetic field strength of 7.05 T. Larmor frequency was 78.89 MHz. The ordinary single pulse sequence was used in which the pulse width was set at 2.8 s and the acquisition time was 0.026 s. The spectral width was 500 kHz. The number of scans was adjusted from 200 to 15,000, depending on the concentration of vanadium. The signal was acquired from the time point 4 μs after the end of the pulse. The sample was static, and its temperature was ambient (294 K). The spectra were expressed with the signal of $VOCl_3$ being 0 ppm, and the higher frequency shift from the standard was positive. Practically, solid NH_4VO_3 (-571.5 ppm) was used as the second external reference.[25]

Results and Discussion

Infrared Spectra. Figure 1 shows IR spectra of V_2O_5/TiO_2-ZrO_2 catalysts with various content calcined at 773 K for 3 h. Although with samples below 25 wt % of V_2O_5 the definite peaks were not observed, the absorption bands at 1022 and 820 cm^{-1} appeared for 25-V_2O_5/TiO_2-ZrO_2, 33-V_2O_5/TiO_2-ZrO_2, and pure V_2O_5 containing high V_2O_5 content. The band at 1022 cm^{-1} is assigned to the V=O stretching vibration, whereas the band at 820 cm^{-1} is attributed to the coupled vibration between V=O and to V-O-V.[26] Generally, the IR band of V=O in crystalline V_2O_5 shows at 1020-1025 cm^{-1} and the Raman band at 995 cm^{-1}.[2,27] The intensity of the V=O absorption gradually decreased with decreasing V_2O_5 content, although the band position did not change. As shown in Figure 1, the catalysts at vanadia loadings below 25 wt % gave no absorption bands from crystalline V_2O_5. This observation suggests that vanadium oxide below 25 wt % is in a highly dispersed state. It is reported that V_2O_5 loading exceeding the formation of monolayer on the surface of support is well crystallized and observed in the spectra of IR and [51]V solid state NMR.[28]

As shown in Figure 1, for samples below 25 wt% of V_2O_5 calcined at 773 K the crystalline V_2O_5 was not observed in their IR spectra, suggesting the monolayer dispersion of V_2O_5 on the surface of TiO_2-ZrO_2 as the amorphous phase. However, it is necessary to examine the formation of crystalline V_2O_5 as a function of calcination temperature. Variations of IR spectra against calcination temperature for 10-V_2O_5/TiO_2-ZrO_2 are shown in Figure 2. For the sample, there are no V=O stretching bands at 1022 cm^{-1} from the calcination temperature of 673 K to 1073 K, indicating no

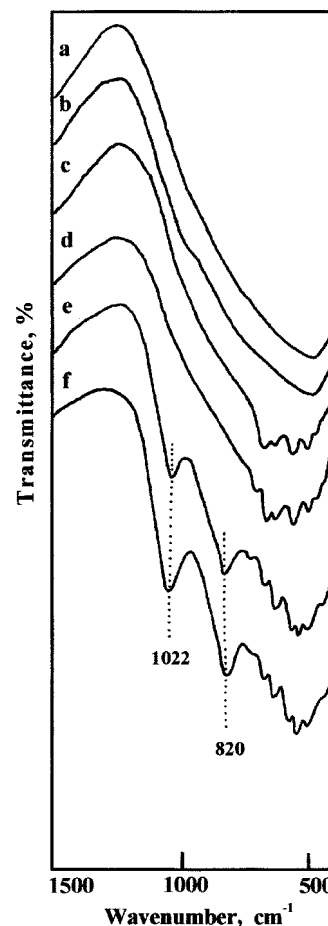**Figure 1**. Infrared spectra of catalysts calcined at 773 K: (a) TiO_2-ZrO_2, (b) 5-V_2O_5/TiO_2-ZrO_2, (c) 10-V_2O_5/TiO_2-ZrO_2, (d) 15-V_2O_5/TiO_2-ZrO_2, (e) 25-V_2O_5/TiO_2-ZrO_2, (f) 33-V_2O_5/TiO_2-ZrO_2, and (g) V_2O_5.

Figure 2. Infrared spectra of 10-V_2O_5/TiO_2-ZrO_2 calcined at (a) 673 K, (b) 773 K, (c) 873 K, (d) 973 K, (e) 1073 K, and (f) 1173 K.

[51]V NMR and IR Study of V₂O₅/TiO₂-ZrO₂

Bull. Korean Chem. Soc. **2000**, Vol. 21, No. 9   915

formation of crystalline V_2O_5. However, as shown in Figure 2, V=O stretching bands due to crystalline V_2O_5 at 1173 K appeared at 1022 cm^{-1} together with lattice vibration bands of V_2O_5 and TiO_2-ZrO_2 below 900 cm^{-1}.[29,30] The formation of crystalline V_2O_5 at 1173 K can be explained in terms of the decomposition of $V_3Ti_6O_{17}$ compound, which was formed through the reaction of V_2O_5 and TiO_2 at 973-1073 K. In the present work, the triclinic phase of crystalline $V_3Ti_6O_{17}$ was confirmed by X-ray diffraction. X-ray diffraction patterns showed the triclinic phase of $V_3Ti_6O_{17}$ (2θ : 27.6, 28.3, 28.4, 36.2, and 41.4°) in the samples calcined at 973-1073 K, and for sample calcined at 1173 K the $V_3Ti_6O_{17}$ phase disappeared due to the decomposition of $V_3Ti_6O_{17}$, leaving the V_2O_5 phase and the rutile phase of TiO_2. These results are in good agreement with those of ^{51}V solid state NMR described later.

Figure 3 shows IR spectra of 25-V_2O_5/TiO_2-ZrO_2 catalysts calcined at 673-1173 K for 3 h. Unlike 10-V_2O_5/TiO_2-ZrO_2 for 25-V_2O_5/TiO_2-ZrO_2 crystalline V_2O_5 appeared at lower calcination temperature from 673 K to 873 K and consequently V=O stretching band was observed at 1022 cm^{-1}. This is because V_2O_5 loading exceeding the formation of monolayer on the surface of ZrO_2 is well crystallized.[28] However, at 973-1073 K all V_2O_5 reacted with ZrO_2 or TiO_2 and changed into ZrV_2O_7 or $V_3Ti_6O_{17}$ so that V=O stretching
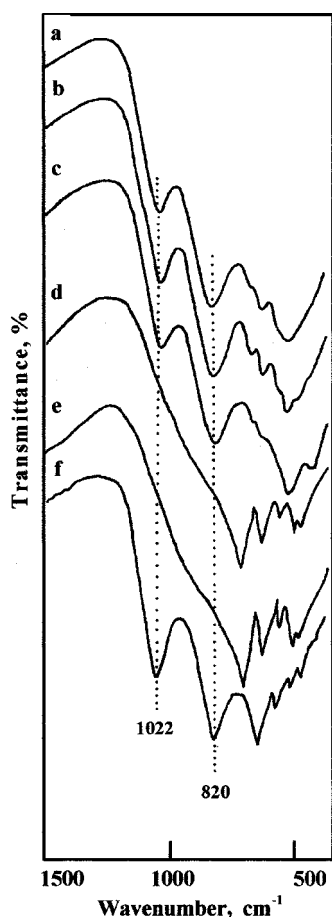
at 1022 cm^{-1} disappeared completely, as shown in Figure 3. At the calcination temperature of 1173 K some of the $V_3Ti_6O_{17}$ decomposed into V_2O_5 and TiO_2, and then the V=O stretching band due to the crystalline V_2O_5 was again observed at 1022 cm^{-1}. These results are in good agreement with those of ^{51}V solid state NMR.

^{51}V Solid State NMR Spectra. Solid state NMR methods represent a novel and promising approach to vanadium oxide catalytic materials. The solid state ^{51}V NMR spectra of V_2O_5/TiO_2-ZrO_2 catalysts calcined at 773 K are shown in Figure 4. There are three types of signals in the spectra of catalysts, with varying intensities depending on V_2O_5 content. At low loadings or up to 15 wt% V_2O_5 a shoulder at about -260 ppm and the intense peak at -590 ~ -730 ppm are observed. The former is assigned to the surface vanadium-oxygen structures surrounded by a distorted octahedron of oxygen atoms, and the latter is attributed to the tetrahedral vanadium-oxygen structures.[31-33]

However, the surface vanadium oxide structure is remarkably dependent on the metal oxide support material. Vanadium oxide on TiO_2 (anatase) displays the highest tendency to be 6-coordinated at low surface coverages, whereas in the case of γ-Al_2O_3 a tetrahedral surface vanadium species is the favored.[32] As shown in Figure 4, at low vanadium loading on TiO_2-ZrO_2 a tetrahedral vanadium species is exclusively dominant compared with a octahedral species. In general, it is known that low surface coverages favor a tetrahedral coordination of vanadium oxide, but at higher surface coverages vanadium oxide becomes increasingly octahedral-coordinated. As shown in Figure 4, the peak shapes for the vana-
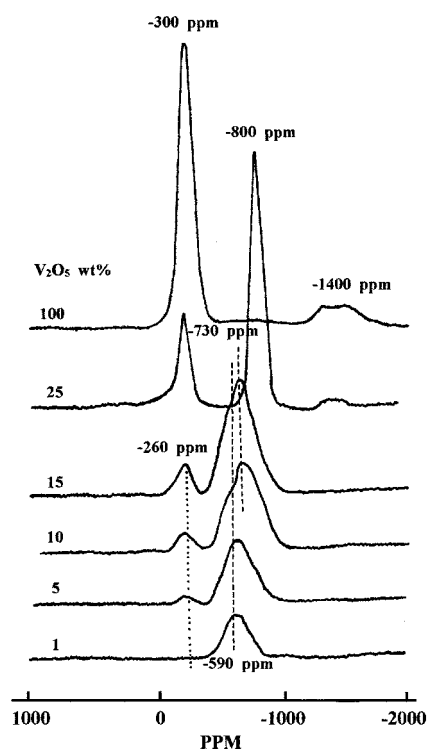
Figure 3. Infrared spectra of 25-V_2O_5/TiO_2-ZrO_2 calcined at (a) 673 K, (b) 773 K, (c) 873 K, (d) 973 K, (e) 1073 K, and (f) 1173 K.

Figure 4. Solid state ^{51}V NMR spectra of V_2O_5/TiO_2-ZrO_2 catalysts calcined at 773 K.

dium species on TiO_2-ZrO_2 are narrower and more symmetric compared with those of vanadium species on TiO_2 or γ-Al_2O_3 reported in other studies.[32,33] It seems likely that the different physical and chemical properties of TiO_2-ZrO_2 compared with TiO_2 or γ-Al_2O_3 affect the symmetry of the surface vanadium-oxygen structures.

Increasing the V_2O_5 content on the TiO_2-ZrO_2 surface changes the shape of the spectrum to a rather intense and sharp peak at about -300 ppm ($\delta_\perp$) and a broad low-intensity peak at about -1400 ppm($\delta_\parallel$), which are due to the crystalline V_2O_5 of square pyramid coordination.[32] These observations of crystalline V_2O_5 for samples containing high V_2O_5 content above 15 wt % are in good agreement with the results of the IR spectra in Figure 1. Namely, this is because V_2O_5 loading exceeding the formation of monolayer on the surface of TiO_2-ZrO_2 is well crystallized.[28]

However, for 25-V_2O_5/TiO_2-ZrO_2 a sharp peak at -800 ppm due to crystalline ZrV_2O_7 appeared, indicating the formation of a new compound from V_2O_5 and ZrO_2. Other investigators[22,31] reported the formation ZrV_2O_7 from V_2O_5 and ZrO_2 at the calcination temperature of 873 K for 1.5 h. In this case, since the sample was prepared by calcining for 3 h, it seems likely that the formation of ZrV_2O_7 occurred even at 773 K of calcination temperature. As discussed below, the cubic phase of ZrV_2O_7 was confirmed by X-ray diffraction. Moreover, the increase in V_2O_5 content resulted in the appearance of additional signals with a peak at -730 ppm. The intensity of the signal increases with increase in V_2O_5 loading. Different peak positions normally indicate differences in the spectral parameters and are observed due to different local environments of vanadium nuclei.[32-36] Thus,

species at -590 ppm and -730 ppm can be attributed to two types of tetrahedral vanadium complexes with different oxygen environments. Namely, the signals at -590 ppm can be attributed to the surface vanadium complexes containing OH groups or water molecules in their coordination sphere,[33] because the evacuation treatment decreases the intensities remarkably. On the other hand, the signals at -730 ppm are due to the surface tetrahedral vanadium complexes, which do not contain OH groups or adsorbed water molecules.

It is necessary to examine the effect of calcination temperature on the surface vanadium oxide structure. The spectra of 10-V_2O_5/TiO_2-ZrO_2 containing lower vanadium oxide content and calcined at various temperatures are shown in Figure 5. The shape of the spectrum is very different depending on the calcination temperature. For the sample calcined at lower temperatures (673-773 K), there are two peaks at about -260 ppm and -590 ~ -730 ppm, a result of the octahedral and tetrahedral vanadium-oxygen structures, indicating the monolayer dispersion of V_2O_5 on the ZrO_2 surface, which are in good agreement with the results of IR spectra of Figure 2. However, for samples calcined at 873 K, only a sharp peak at -800 ppm, due to crystalline ZrV_2O_7, appeared, indicating that most of V_2O_5 on the surface of TiO_2-ZrO_2 was consumed to form the ZrV_2O_7 compound. For sample calcined at 873 K, X-ray diffraction patterns for the cubic phase of ZrV_2O_7 (2θ : 20.0, 33.9, 46.3, 52.8, and 54.5°) were observed. At 973-1073 K calcination temperatures, we also observed only a sharp peak at -800 ppm. For samples calcined at 973-1073 K, X-ray diffraction patterns of $V_3Ti_6O_{17}$ were observed. In previous work[22] it was known
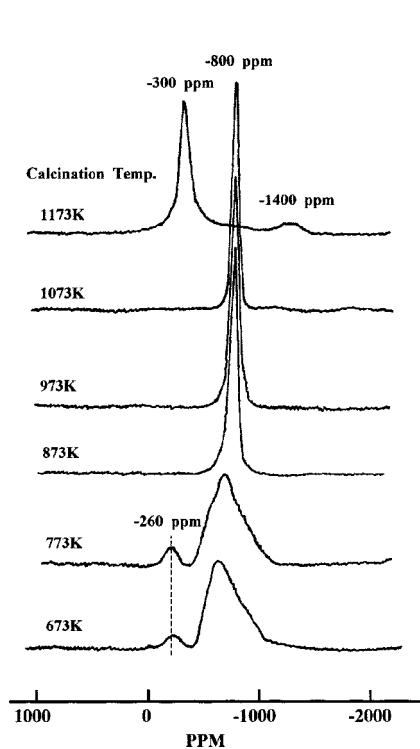

Figure 5. Solid state ^{51}V NMR spectra of 10-V_2O_5/TiO_2-ZrO_2 calcined at different temperatures.

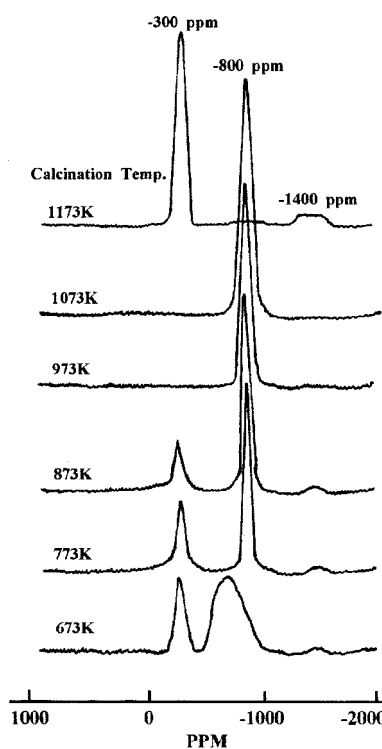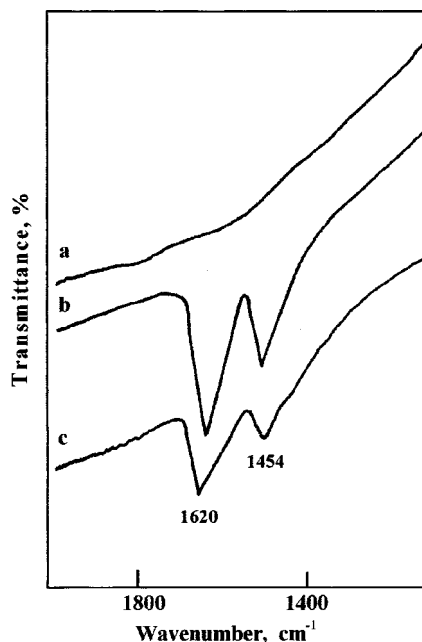**Figure 6**. Solid state ^{51}V NMR spectra of 25-V_2O_5/TiO_2-ZrO_2 calcined at different temperatures.

Figure 7. Infrared spectra of NH_3 adsorbed on $10\text{-}V_2O_5/TiO_2\text{-}ZrO_2$ calcined at 973 K.: (a) background of $10\text{-}V_2O_5/TiO_2\text{-}ZrO_2$ evacuated at 673 K for 1 h, (b) NH_3 (20 torr) adsorbed on (a), and (c) b sample evacuated at 503 K for 0.5 h.

that the ZrV_2O_7 compound decomposed completely to V_2O_5 and ZrO_2 at 1073 K. Therefore, on the basis of previous work and the present result it is clear that a sharp peak at -800 ppm for $10\text{-}V_2O_5/TiO_2\text{-}ZrO_2$ calcined at 1073 K is due to the crystalline $V_3Ti_6O_{17}$ phase formed by the reaction between V_2O_5 and TiO_2. However, at 1173 K of calcination temperature we observed only the peaks of crystalline V_2O_5 at -300 ppm and about -1400 ppm, indicating the decomposition of $V_3Ti_6O_{17}$. These results are in good agreement with those of IR spectra in Figure 2.

The spectra of $25\text{-}V_2O_5/TiO_2\text{-}ZrO_2$ containing higher vanadium oxide content than monolayer loading and calcined at various temperatures are shown in Figure 6. Unlike $10\text{-}V_2O_5/TiO_2\text{-}ZrO_2$, for $25\text{-}V_2O_5/TiO_2\text{-}ZrO_2$ calcined even at the lower temperature of 673 K a sharp peak due to crystalline V_2O_5 appeared at -300 ppm and -1400 ppm together with a peak at -590 ~ -730 ppm due to the tetrahedral surface species. However, the for sample calcined at 773 K, in addition to a peak at -300 ppm due to crystalline V_2O_5, a sharp peak at -800 ppm due to ZrV_2O_7 compound appeared. As shown in Figure 6, the peak intensity of ZrV_2O_7 increased with an increase in calcination temperature, consuming the content of crystalline V_2O_5. Consequently, at 973 K of calcination temperature only a peak due to the ZrV_2O_7 and $V_3Ti_6O_{17}$ phases appeared at -800 ppm. As mentioned above, since at 1073 K the ZrV_2O_7 decomposes completely to V_2O_5 and ZrO_2, a sharp peak at -800 ppm for $25\text{-}V_2O_5/TiO_2\text{-}ZrO_2$ calcined at 1073 K is due to the crystalline $V_3Ti_6O_{17}$ phase. At the calcination temperature of 1173 K a sharp peak of crystalline V_2O_5 at -300 ppm due to the decomposition of $V_3Ti_6O_{17}$ was again observed.

Acidic Properties. Infrared spectroscopic studies of ammonia adsorbed on solid surfaces have made it possible to distinguish Brönsted acid sites from Lewis acid sites.[22,37] Figure 7 shows the IR spectra of ammonia adsorbed on $10\text{-}V_2O_5/TiO_2\text{-}ZrO_2$ calcined at 973 K and evacuated at 673 K for 1 h. For $10\text{-}V_2O_5/TiO_2\text{-}ZrO_2$ the bands at 1454 cm^{-1} are the characteristic peaks of ammonium ion, which are formed on the Brönsted acid sites and the bands at 1620 cm^{-1} are contributed by ammonia coordinately bonded to Lewis acid sites,[22,37] indicating the presence of both Brönsted and Lewis acid sites. Other samples having different vanadium content also showed the presence of both Lewis and Brönsted acids. Therefore, these $V_2O_5/TiO_2\text{-}ZrO_2$ samples can be used as catalysts for Lewis or Brönsted acid catalysis.

Conclusions

This paper shows that a combination of FTIR and ^{51}V solid-state NMR can be used to perform the characterization of V_2O_5 catalysts supported on $TiO_2\text{-}ZrO_2$. On the basis of results of FTIR and solid state ^{51}V NMR, at low calcination temperature of 773 K up to 15 wt% of vanadium oxide was well dispersed on the surface of $TiO_2\text{-}ZrO_2$. However, high V_2O_5 loading (equal to or above 25 wt%) exceeding the formation of monolayer on the surface of $TiO_2\text{-}ZrO_2$ was well crystallized. The ZrV_2O_7 compound was formed through the reaction of V_2O_5 and ZrO_2 at 773-973 K, whereas the $V_3Ti_6O_{17}$ compound was formed through the reaction of V_2O_5 and TiO_2 at 973-1073 K. The $V_3Ti_6O_{17}$ decomposed to V_2O_5 and TiO_2 at 1173 K, which were confirmed by FTIR and ^{51}V NMR. Infrared spectroscopic studies of ammonia adsorbed on $V_2O_5/TiO_2\text{-}ZrO_2$ catalysts showed the presence of both Lewis and Brönsted acids.

References

1. Nakagawa, Y.; Ono, T.; Miyata, H.; Kubokawa, Y. *J. Chem. Soc., Faraday Trans. 1* **1983**, *79*, 2929.
2. Miyata, H.; Kohno, M.; Ono, T.; Ohno, T.; Hatayama, F. *J. Chem. Soc. Faraday Trans. 1* **1989**, *85*, 3663.
3. Reddy, B. M.; Ganesh, I.; Chowdhury, B. *Catal. Today* **1999**, *49*, 115.
4. Lakshmi, L. J.; Ju, Z.; Alyea, E. C. *Langmuir* **1999**, *15*, 3521.
5. Doh, I. J.; Pae, Y. I.; Sohn, J. R. *J. Ind. Eng. Chem.* **1999**, *5*, 161.
6. Forzatti, P.; Tronoconi, E.; Busca, G.; Titarellp, P. *Catal. Today* **1987**, *1*, 209.
7. Busca, G.; Elmi, A. S.; Forzatti, P. *J. Phys. Chem.* **1987**, *91*, 5263.
8. Centi, G.; Militerno, S.; Perathoner, S.; Riva, A.; Barambilla, G. *J. Chem. Soc., Chem. Commun.* **1991**, 88.
9. Centi, G.; Perathoner, S.; Kartheuser, B.; Rohan, D.; Hoidnett, B. K. *Appl. Catal. B* **1992**, *1*, 129.
10. Matralis, H. M.; Ciardelli, M.; Ruwet, M.; Grange, P. *J.*

Catal. **1995**, *157*, 368.

11. Mastikhin, V. M.; Terskikh, V. V.; Lapina, O. B.; Filiminova, S. V.; Seidl, M.; Knovinger, H. *J. Catal.* **1995**, *156*, 1.
12. Elmi, A. S.; Tronoconi, E.; Cristiani, C.; Martin, J. P. G.; Forzatti, P. *Ind. Eng. Chem. Res*. **1989**, *84*, 237.
13. Miyata, H.; Fujii, K.; Ono, T.; Kubokawa, Y.; Ohno, T.; Hatayama, F. *J. Chem. Soc., Faraday Trans. 1* **1987**, *83*, 675.
14. Cavani, F.; Centi, G.; Foresti, E.; Trifiro, F. *J. Chem. Soc., Faraday Trans. 1* **1988**, *84*, 237.
15. Hayata, F.; Ohno, T.; Maruoka, T.; Miyata, H. *J. Chem. Soc., Faraday Trans*. **1991**, *87*, 2629.
16. del Arco, M.; Holgado, M. J.; Martin, C.; Rives, V. *Langmiur* **1990**, *6*, 801.
17. Centi, G.; Pinelli, D.; Trifiro, F.; Ghoussoub, D.; Guelton, M.; Gengembre, L. *J. Catal.* **1991**, *130*, 238.
18. Inomata, M.; Mori, K.; Miyamoto, A.; Murakami, Y. *J. Phys. Chem.* **1983**, *87*, 761.
19. Scharf, U.; Schraml-Marth, M.; Wokaun, A.; Baiker, A. *J. Chem. Soc., Faraday Trans.* **1991**, *87*, 3299.
20. Miyata, H.; Kohno, M.; Ono, T.; Ohno, T.; Hatayama, F. *J. Mol. Catal*. **1990**, *63*, 181.
21. Sohn, J. R.; Park, M. Y.; Pae, Y. I. *Bull. Korean Chem. Soc*. **1996**, *17*, 274.
22. Sohn, J. R.; Lee, M. H.; Doh, I. J.; Pae, Y. I. *Bull. Korean Chem. Soc*. **1998**, *19*, 856.
23. Kera, Y.; Hirota, K. *J. Phys. Chem*. **1969**, *73*, 3937.
24. Cole, D. J.; Cullis, C. F.; Hucknall, D. J. *J. Chem. Faraday Tran. 1* **1976**, *72*, 2185.
25. Hayashi, S.; Hayamizu, K. *Bull. Chem. Soc. Jpn.* **1990**, *63*, 961.
26. Mori, K.; Miyamoto, A.; Murakami, Y. *J. Chem. Soc., Faraday Trans.* **1987**, *83*, 3303.
27. Bjorklund, R. B.; Odenbrand, C. U. I.; Brandin, J. G. M.; Anderson, L. A. H.; Liedberg, B. *J. Catal.* **1989**, *119*, 187.
28. Sohn, J. R.; Cho, S. G.; Pae, Y. I.; Hayashi, S. *J. Catal.* **1996**, *159*, 170.
29. Inomata, M.; Miyamoto, A.; Marakami, Y. *J. Catal.* **1980**, *62*, 140.
30. Highfield, J. G.; Moffat, J. B. *J. Catal.* **1984**, *88*, 177.
31. Roozeboom, F.; Mittelmelijer- Hazeleger, M. C.; Moulijn, J. A.; Medema, J.; de Beer, U. H. J.; Gelling, P. J. *J. Phys. Chem.* **1980**, *84*, 2783.
32. Eckert, H.; Wachs, I. E. *J. Phys. Chem*. **1989**, *93*, 6796.
33. Reddy, B. M.; Reddy, E. P.; Srinivas, S. T.; Mastikhim, V. M.; Nosov, N. V.; Lapina, O. B. *J. Phys. Chem.* **1992**, *96*, 7076.
34. Le Costumer, L. R.; Taouk, B.; Le Meur, M.; Payen, E.; Guelton, M.; Grimblot, J. *J. Phys. Chem.* **1988**, *92*, 1230.
35. Narsimha, K.; Reddy, B. M.; Rao, P. K.; Mastikhin, V. M. *J. Phys. Chem.* **1990**, *94*, 7336.
36. Sobalik, Z.; Lapina, O. B.; Novgorodova, O. N.; Mastikhin, V. M. *Appl. Catal.* **1990**, *63*, 191.
37. Satsuma, A.; Hattori, A.; Mizutani, K.; Furuta, A.; Miyamoto, A.; Hattor, T.; Murakami, Y. *J. Phys. Chem.* **1988**, *92*, 6052.